JNPS 10 (2): 8-18 (2024)
ISSN: 2392-473X(Print), 2738-9537 (Online)

Research Article ©Nepal Physical Society
doi.org/10.3126/jnphyssoc.v10i2.79470

Study of The Molecular Structure, Electronic Structure, Spectroscopic Analysis and Thermodynamic Properties of Dibenzofuran Using First Principles

Roshika Uprety[1], Rabin Ghimire[1], Pima Gharti Magar[1], Dilip Rokka[1], Ishwor Bahadur Khadka[2], Rajendra Neupane[3], Krishna Bahadur Rai[1,*]

[1]Department of Physics, Patan Multiple Campus, Lalitpur, Tribhuvan University, Nepal
[2]Division of Physics Semiconductor Science, Dongguk University, Seoul, Republic of Korea
[3]Department of Physics, Birendra Multiple Campus, Chitwan, Tribhuvan University, Nepal

[*]Corresponding author email: krishnarai135@gmail.com

Abstract

This study examines the different properties of dibenzofuran using density functional theory (DFT) B3LYP/6-311G(d, p) basis set. In dibenzofuran molecules, seven steps are required to establish an optimized energy setup. The HOMO-LUMO energy gap is found to be 5.028 eV. The value of global reactivity parameters i.e. chemical potential (μ), electronegativity (χ), global hardness (η), global softness (ζ) and electrophilicity (ω) are found to be - 3.751 eV, 3.751 eV, 2.514 eV, 0.398 $(eV)^{-1}$ and 2.798 eV respectively. The observed energy gap in the DOS spectrum for the dibenzofuran is 4.992 eV which is almost equal to the HOMO-LUMO energy gap. Mulliken charges with the C3 and C7 atoms are observed with the highest positive charges along with some positive charges on all the hydrogens atoms while oxygen O21 shows the highest negative charge together with some negative charges on C1, C2, C4, C5, C6, C8, C9, C10, C11 and C12 atoms. The MEP and ESP showed that there is negative potential localized around the benzene ring and oxygen atom showing nucleophilic region. In contrast, the positive potential is localized around the hydrogen atom showing an electrophilic region. Electron density shows the uniform charge distribution. The observed peak values for the C-C vibrations are at 1471 cm^{-1} and 1484 cm^{-1}, C-H vibration are at 3191 cm^{-1}, and C-O vibration is at 1215 cm^{-1}. Thermodynamic parameters like heat capacity at constant volume and constant pressure, internal energy, enthalpy and entropy increase with the rise in temperature i.e. from 10 K to 500 K and Gibbs free energy decreases with the same increase in temperature.

Keywords: Density functional theory, HOMO-LUMO, Molecular electrostatic potential, IR-Spectroscopy, Thermodynamic properties

Submitted: October 20, 2024; **Revised:**May 26,2025; Acceped: June 01,2025

Introduction

Dibenzofuran (DBF) is the heterocyclic aromatic compound along with oxygen and its molecular formula is $C_{12}H_8O$. Figure 1 shows the Chemical structure of dibenzofuran. It gets dissolved in a non-polar organic solvent and is a volatile white solid [1]. Dibenzofuran is known to be found in bituminous coal [2]. It is

eco-toxic heterocyclic compound which is also produced by burning a variety of nanomaterials, also found in cigarette ash. Mostly the general public is exposed to it through contaminated food and water, industrial chemical waste, combustion, and industrial chemical processes [3, 4]. The several derivative of dibenzofuran are extensively used in medical science. Many biological activities were shown by them, including anti-inflammatory, anti-platelet, anti-cancer, anti-bacterial, anti-fungal, anti-malarial, anti-allergic, and anti-HIV-1 agent properties [5].

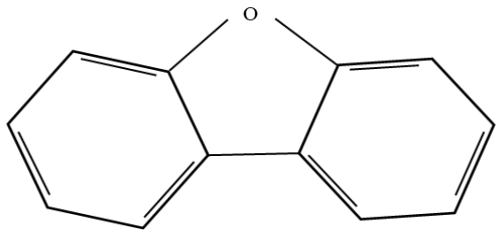

Figure 1: Chemical structure of dibenzofuran

On spanning of time, Li et al., studied the gas phase formation mechanism of different compounds including dibenzofuran and he also explored the reaction of benzofuran, with cyclopentadienyl radical (CPDyl) to form dibenzofuran [6]. The work on the synthesis and characterization of organic dyes from dibenzofuran for the use in dye-sensitized solar cells were focused by Periyasamy et al., [7]. From the results of various investigations, formation of polychlorinated dibenzo-p-dioxins/ dibenzofurans from a refinery process for zinc oxide [8-10] was used in feed additives. Researchers found the structure, and electronic spectra of dibenzofuran together with its polychlorinated derivative [11]. Lee reported about the dibenzofuran in both the ground and lowest triplet state employing Density Functional Theory (DFT) with the 6-31G* basis set to investigate the molecular geometries, excitation energies, and vibrational frequencies [12].

In the past, many researches performed on dibenzofuran have revealed different characteristics that are useful for different applications. However, the complete study of molecular structure, spectroscopic analysis, electronic structure and thermodynamic properties of the dibenzofuran molecule has not been performed so far. So, this study addresses about the optimization energy, highest occupied molecular orbital and lowest unoccupied molecular orbital (HOMO-LUMO) energy gap, global reactivity index (GRI), density of states (DOS), Mulliken atomic charge, electrostatic potential (ESP), molecular electrostatic potential (MEP), electron density (ED), IR- spectroscopy, and thermodynamic properties analysis of dibenzofuran using DFT with B3LYP method at 6-311G (d, p) basis set.

2. Computational Methodology

The quantum calculation of dibenzofuran molecule was performed using Gaussian09W program together with GaussView v6.0. At first, the most optimized structure of the title molecule was determined followed by the visualization/calculation of highest occupied molecular orbital and lowest unoccupied molecular orbital (HOMO-LUMO), global reactivity index, Mulliken charges, MEP, ESP, ED and vibrational characteristics (FT-IR), using the density functional theory (DFT) B3LYP method at 6-311G (d, p) basis set. Density of state (DOS)

spectrum was obtained employing the .log file into the GaussSum3.0 program. The relation of thermodynamic parameters such as heat capacity at constant volume (C_V), heat capacity at constant pressure (Cp), total internal energy (U), enthalpy (H), entropy (S) and Gibb's free energy (G) were determined with change in temperature was were calculated using Moltran software for the .log file from the Gaussian software.

Koopman's theorem suggested that HOMO and LUMO energies are directly associated with ionization potential (I) and electron affinity (A) respectively. Ionization energy (I) is the amount of energy needed to remove an electron from a gaseous atom. Similarly, electron affinity (A) is a measure of the energy released when an extra electron is added to an atom. The relation for ionization potential (I) and electron affinity (A) are shown below [13].

$$\text{Ionization Potential (I)} = -E_{HOMO} \quad (1)$$

$$\text{Electron Affinity (A)} = -E_{LUMO} \quad (2)$$

The relation for chemical Potential (μ) and electronegativity (χ) are shown below respectively [14].

$$\text{Chemical potential } (\mu) = -(I+A)/2 \quad (3)$$

$$\text{Electronegativity } (\chi) = (I+A)/2 \quad (4)$$

Similarly, the global hardness of the molecule is expressed as,

$$\text{Global Hardness } (\eta) = (I-A)/2 \quad (5)$$

The multiplicative inverse of global hardness is softness which is expressed as,

$$\text{Softness } (\zeta) = 1/\eta \quad (6)$$

Furthermore, the relation for electrophilicity index (ω) is shown below [15].

$$\text{Electrophilic Index } (\omega) = \mu^2/2\eta \quad (7)$$

3. Results and Discussion

3.1 Optimized molecular structure and visualization of optimization steps

The ground state optimized geometry of dibenzofuran ($C_{12}H_8O$) molecule is displayed in Figure 2(a), along with name and atomic numbering. Optimization energy is the lowest energy for a given molecular structure. Energy minimization is the essential process to set the proper molecular arrangement. The results of the total energy optimization process steps of $C_{12}H_8O$ molecule is shown in Figure 2(b), illustrating the relation between total energy versus optimization step number. Here Figure 2(b) shows the total optimization of energy that occurs in seven distinct steps. It is seen that the optimization of dibenzofuran has begun from energy of -537.382 Hartree. In first two steps, the energy abruptly decreases up to -537.455 Hartree. Again the energy decreases gradually and reaches to -537.456 Hartree which is the optimized energy of dibenzofuran.

(a)

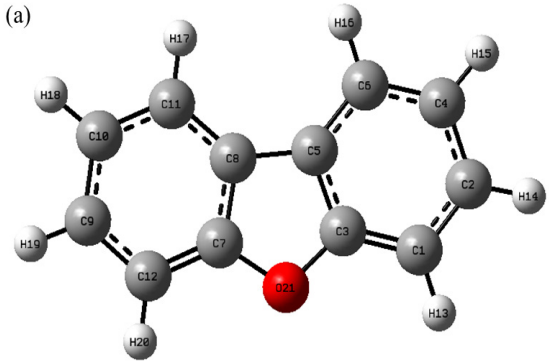

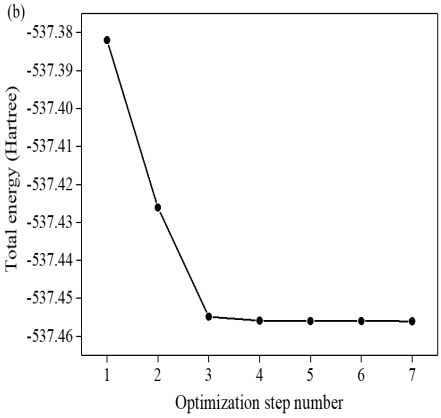

Figure 2: (a) Optimized structure and (b) Plot for optimization step number vs total energy of dibenzofuran

3.2 Highest Occupied Molecular Orbitals (HOMO) and Lowest Unoccupied Molecular Orbital (LUMO) analysis

The highest energy orbitals with electron that have the potential to donate electron is termed as HOMO. The lowest energy orbitals which can serve as the electron acceptor is known as LUMO. The ionization potential and electron affinity are directly related to HOMO and LUMO respectively. High HOMO energy suggests that it has higher tendency to donate electron and vice versa whereas the lower LUMO energy value denotes the greater chance of accepting electron. The energy difference between HOMO and LUMO is essential index which is used to determine electron conductivity (mobility). A lower gap value denotes a higher electrical transition and vice versa [16]. Figure 3 shows the energies of two molecular orbitals i.e. HOMO and LUMO of dibenzofuran with their respective values - 6.265 eV and - 1.237 eV and the Energy gap (ΔE) = E_{LUMO} - E_{HOMO} = 5.028 eV.

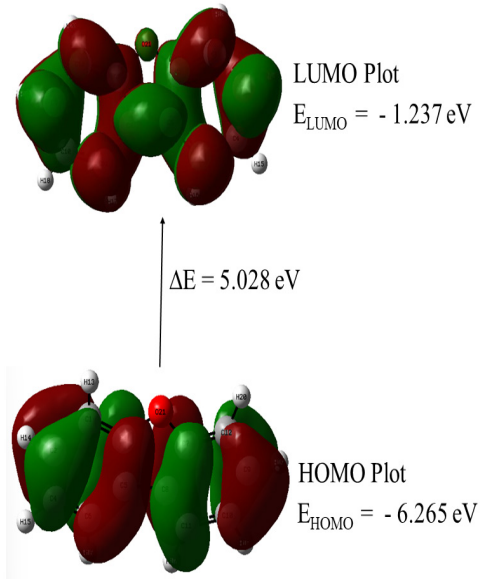

Figure 3: The atomic orbital compositions of the frontier molecular orbital (HOMO-LUMO)

3.3 Global reactivity parameter

This study offers a variety of chemical reactivity indicators in an effort to improve our understanding of the characteristics of $C_{12}H_8O$. Global reactivity parameter such as ionization potential (I), electron affinity (A), chemical potential (μ), electronegativity (χ), hardness (η), softness (ζ) and electrophilicity index (ω) for the dibenzofuran molecule were evaluated. The value for Ionization Potential (I) = $-E_{HOMO}$ and Electron Affinity (A) = $-E_{LUMO}$ are found to be 6.265 eV and 1.237 eV respectively for dibenzofuran. Also, the high value for the HOMO-LUMO energy gap (i.e. 5.028 eV) suggests the hardness of given molecule. Chemical Potential (μ) and electronegativity (χ) (negative of chemical potential) provide information about the nature of chemical interaction.

The value for the Chemical potential (μ) and Electronegativity (χ) are found to be -3.751 eV and 3.751 eV respectively. The negative value of chemical potential for dibenzofuran indicates that the molecule has high stability and doesn't decompose. The value for global hardness (η) and softness (ζ) for dibenzofuran are 2.514 eV and 0.398 $(eV)^{-1}$ respectively which indicates that the dibenzofuran is hard. The global electrophilicity index (ω) measures the molecule's ability to donate electrons. The value for the electrophilic Index (ω) for dibenzofuran is found to be 2.798 eV which is greater than 1.5 eV indicating strong electrophile.

3.4 Density of States (DOS)

Figure 4 shows the density of states (DOS) spectrum of the dibenzofuran molecule obtained using the GaussSum 3.0 program.

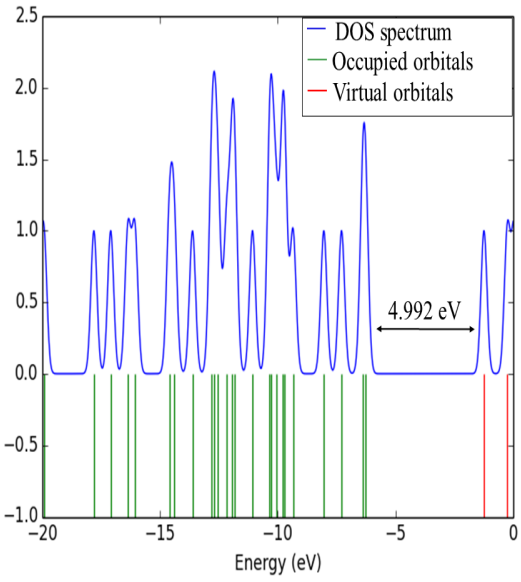

Figure 4: DOS spectrum of dibenzofuran molecule

This spectrum is helpful in describing how electrons take part in conduction and valence bands, and also insights about degeneracy (states having same energy level). As the intensity increases, there will be plenty of state available for the occupation in the specific energy level while the zero DOS intensity implies no states are there for occupation by the system [17]. In the figure 4, the energy range denoted by green color is known to be occupied, filled, and donor orbitals while the energy range denoted by red color is known to be virtual, unfilled, and acceptor orbitals [18]. The observed energy gap in the DOS spectrum for the title molecule is 4.992 eV which is almost equal to the HOMO-LUMO energy gap i.e. 5.028 eV and it shows the good agreement between them.

3.5 Mulliken charge

The idea of electrostatic potential beyond the molecular surface and the process of electronegativity equalization is being defined by Mulliken atomic charge distribution [19]. The Mulliken charge is directly related to the molecule's vibrational characteristics so is co-related with the chemical bonds present in a molecule [20]. Figure 5 shows the Mulliken charge plot of $C_{12}H_8O$. In this plot, we detect that the C3 and C7 have the highest positive charge while the oxygen atom O21 has the highest negative charge. In addition to these, all the hydrogen atoms contain positive charge and C1, C2, C4, C5, C6, C8, C9, C10, C11 and C12 have the negative charges in them.

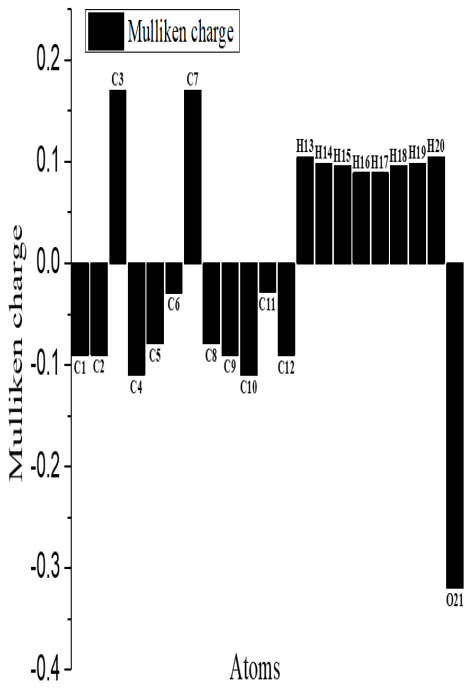

Figure 5: Histogram of Mulliken charge distribution of each atom in dibenzofuran

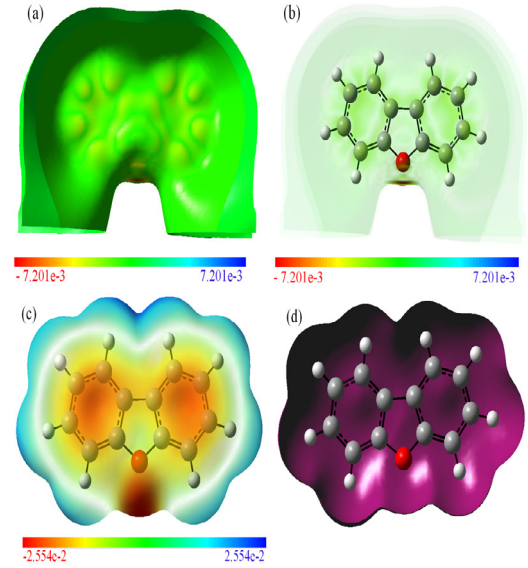

Figure 6: (a) solid view of electrostatic potential (b) transparent view of electrostatic potential (c) molecular electrostatic potential (d) electron density of dibenzofuran

3.6 Electrostatic Potential (ESP), Molecular Electrostatic Potential (MEP), and Electron Density (ED)

Figures 6(a) and 6(b) show the ESP mapped on an iso-density surface in the range of -7.201e-3 (red) to 7.201e-3 (blue). The different values of electrostatic potential at the surface are represented by different colors and increase in the order of red<orange<yellow<green<blue. Here, the region around the oxygen with the red surface (nucleophilic region) suggests the negative potential whereas the positive potential lies on the remaining surface indicating the electrophilic region.

MEP is a very useful tool that helps to understand the electrophilic attack and nucleophilic reaction as well as gives ideas about hydrogen bonding interaction [21]. Figures 6(c) shows the MEP plot of $C_{12}H_8O$ ranging from -2.554e-2 (red) to 2.554e-2 (blue) and this plot provides an overview of the relative polarity of the title molecule and relates their value to electron density (ED) [22]. Various colors have been used to trace MEP surfaces based on ESP. Here red symbolizes the most negative potential, blue denotes the most positive potential, and green symbolizes the zero potential region of the $C_{12}H_8O$ molecule. We observe that in dibenzofuran, negative potential is accumulated around oxygen atom while positive potential is within hydrogen atom. Similarly, negative potential is accumulated

inside the benzene ring. Figure 6(d) corresponds to electron density plot of dibenzofuran and it shows the uniform charge distribution.

3.7 Vibrational analysis

IR spectroscopic analysis is carried out to analyze the vibrational mode of molecular structure. For the molecule with N atoms, the highest number of normal modes of vibration is equal to (3N-6) [23]. There are 21 atoms in the $C_{12}H_8O$ molecule and hence 57 modes of vibration are obtained.

Figure 7 shows the IR spectra of dibenzofuran molecule. The C-C stretching vibrations is supposed to be in between the region 1625-1430 cm^{-1} in aromatic rings [16, 22]. Here the observed peak values of FT-IR spectrum are at in 1471 cm^{-1} and 1484 cm^{-1}. Many aromatic rings have C-H vibrations in the range of 3300-3000 cm^{-1} [16, 22]. For this C-H vibration, FT-IR peak is observed only in 3191 cm^{-1}.The vibration of Carbon Oxygen (C-O) single bond lies in the region of 1300-1000 cm^{-1} [16, 22]. For this C-O vibration, the observed peak value for FT-IR spectrum related to it is 1215 cm^{-1}.

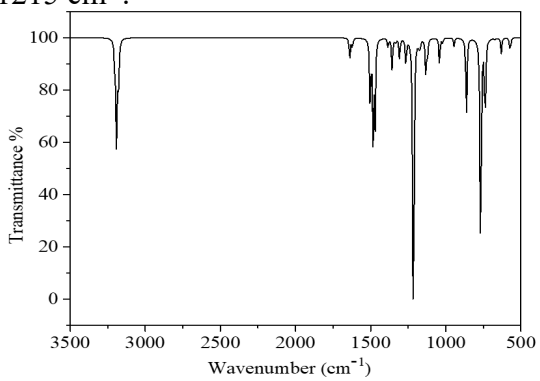

Figure 7: FT-IR-spectra of dibenzofuran using DFT method

3.8 Thermodynamics Properties analysis

The effect of temperature on common statistical thermodynamic functions, including heat capacity at constant volume (C_V), heat capacity at constant pressure (C_p), internal energy (U), enthalpy (H), entropy (S), and Gibbs free energy (G) were calculated using Moltran program [24]. The thermodynamic parameters were obtained based on the vibrational analysis. Figure 8(a) gives us information on how C_v and C_p change with temperature in the range of 10 to 500 K. In this figure, we observe that both C_p and C_V increase with increase in temperature and the experimental observation also support this trend [25]. It is because as the temperature rises, the molecular vibration intensities increase, leading to an increase in C_v and C_p. Internal energy and enthalpy typically rise with temperature [26]. Figure 8(b) shows that the internal energy (U) and enthalpy (H) change along with the rise in temperature. Here both the parameters gradually increase with increasing temperature. This is because the molecular vibration increases with temperature resulting in the increase of U and H. Similarly, Figure 8(c) insight about the relation of entropy (S) and Gibbs free energy (G) with temperature. In this case, entropy (S) sharply increases up to 50K and smoothly increases from 50 K to 500 K. However, it is seen that Gibbs free energy (G) decreases with increase in temperature. It is because Gibbs free energy (G) is related to entropy (S) by the thermodynamic relation $\Delta G = \Delta H - T\Delta S$ [27, 28]. So, as entropy increases, Gibbs free energy decreases along with temperature.

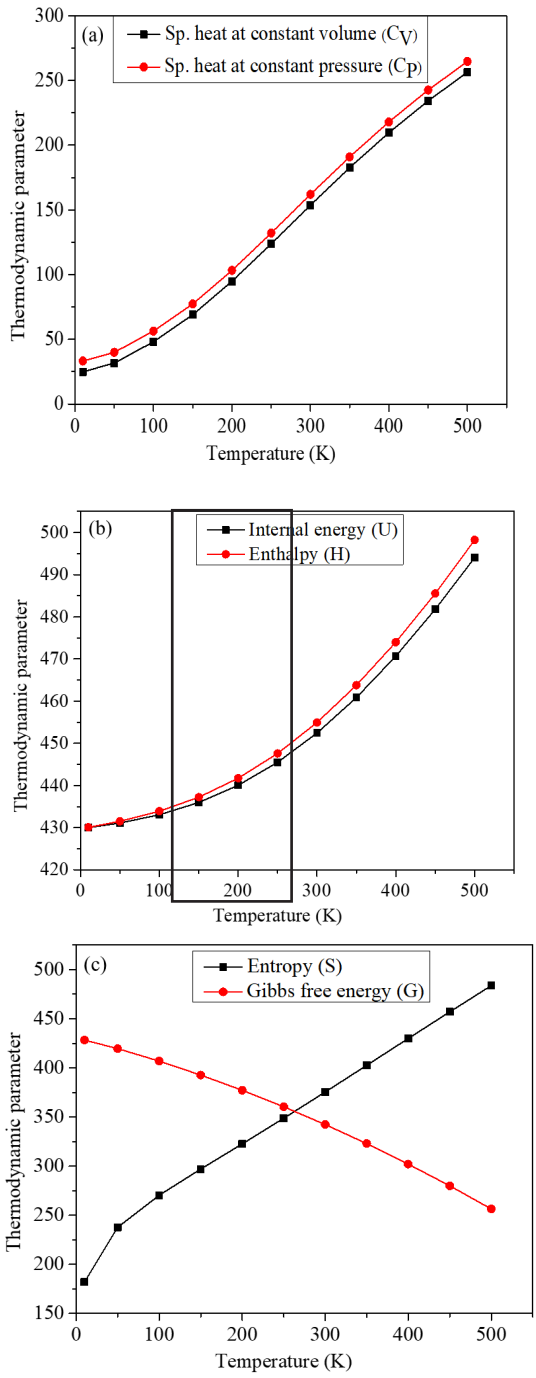

Figure 8: (a) Plots of C_P and C_V vs temperature (b) plot of U and H vs temperature (c) plot of S and G vs temperature

4. Conclusion

In this study we have found molecular geometry, electronic structure, global reactivity parameter, density of states, Mulliken charges, ESP, MEP, ED, vibrational analysis and thermodynamic properties of dibenzofuran using (DFT) B3LYP method at 6-311G (d, p) basis set. Here, the optimization energy state occurs in seven steps. The frontier orbitals (HOMO-LUMO) was studied and their energy gap was found to be 5.028 eV. Similarly, the value for global reactivity parameter such as ionization potential (I), electron affinity (A), chemical potential (μ), electronegativity (χ), hardness (η), softness (ζ) and electrophilicity index (ω) for the dibenzofuran molecule were found to be 6.265 eV, 1.237 eV, -3.751 eV, 3.751 eV, 2.514 eV, 0.398 $(eV)^{-1}$ and 2.798 eV respectively. The energy gap 4.992 eV from spectra of DOS well coordinates with the energy gap observed in the HOMO-LUMO analysis. The Mulliken atomic charges were examined and found that C3 and C7 have the highest positive charge and all the hydrogen atoms contain positive charge while the oxygen atom O21 has the highest negative charge together with some negative charges on C1, C2, C4, C5, C6, C8, C9, C10, C11 and C12 atoms. The nucleophilic and electrophilic reaction sites of the molecule are predicted by the ESP and MEP surface. Here oxygen atom site represents the nucleophilic region while the Hydrogen atom site represents the electrophilic region. Electron density plot of dibenzofuran shows the uniform charge distribution. The observed peak values for the FT-IR spectrum for C-C vibrations are at 1471 cm^{-1} and 1484 cm^{-1}, C-H vibration

is at 3191 cm^{-1}, and C-O vibration is at 1215 cm^{-1}. Relationship between different thermodynamic parameters C_v, $C_{p,}$ U, H, S and G with respect to the change in temperature have been observed and it is found that C_v, C_p, U, H and S increase with rise in temperature from 10 K to 500 K while G decreases with same increase of temperature. Hence the quantum calculation performed in the basis set helps us to better analyze and understand the molecule dynamics and helps in future investigation.

Conflict of interest statement by authors

The authors declare that they have no conflicts of interest.

References

[1] G. Collin and H. Hoke, Ullmann's Encyclopedia of Industrial Chemistry. Wiley, 2000.

[2] R. Hayatsu, R. E. Winans, R. G. Scott, L. P. Moore, and M. H. Studier, "Trapped organic Compounds and aromatic units in coals," Fuel, vol. 57, no. 9, pp. 541-548, 1978, doi: 10.1016/0016-2361(78)90039-X

[3] K. N. Thakore and H. M. Mehendale, "Dibenzofuran," in Encyclopedia of Toxicology, Elsevier B. V., 2005.

[4] K. B. Rai, R. P. Yadav, P. M. Shrestha, S. P. Gupta, R. Neupane, and R.R. Ghimire, "Fabrication of gas sensor based on graphene for the adsorption of gases produced from waste material in kitchen and its surrounding," J. Nepal Phys. Soc., vol. 8, no. 3, pp. 26–31, 2022, doi: 10.3126/jnphyssoc.v8i3.50719

[5] M. R. S. Savanur, A. Kumar, M. Kumar, and S. Kumar, "Medicinal active applications of Dibenzofuran derivatives," Chem. Biol. Lett., vol. 9, no. 4, pp. 374, 2022. https://pubs.thesciencein.org/journal/index.php/cbl/article/view/374

[6] X. Li, Y. Gao, C. Zuo, S. Zheng, F. Xu, Y. Sun, and Q. Zhang, "The Gas-Phase Formation Mechanism of Dibenzofuran (DBF), Dibenzothiophene (DBT), and Carbazole (CA) from Benzofuran (BF), Benzothiophene (BT), and Indole (IN) with Cyclopentadienyl Radical," Int. J. Mol. Sci., vol. 20, no. 21, pp. 5420, 2019, doi: 10.3390/ijms20215420

[7] K. Periyasamy, P. Sakthivel, P. Vennila, P. M. Anbarasan, G. Venkatesh, and Y. Sheena Mary, "Novel D-π-A phenothiazine and dibenzofuran organic dyes with simple structures for efficient dye-sensitized solar cells," J. Photochem. Photobiol. A Chem., vol. 413, pp. 113269, 2021, doi: https://doi.org/10.1016/j.jphotochem.2021.113269

[8] M. K. Kim, D. G. Kim, S. W. Choi, P. Guerrero, J. Norambuena, and G. S. Chung, "Formation of polychlorinated dibenzo-p-dioxins/dibenzofurans (PCDD/Fs) from a refinery process for zinc oxide used in feed additives: A source of dioxin contamination in Chilean pork," Chemosphere, vol. 82, no. 9, pp. 1225–1229, 2011, doi: 10.1016/j.chemosphere.2010.12.040

[9] R. R. Ghimire, Y. P. Dahal, K. B. Rai, and S. P. Gupta, "Determination of Optical Constants and Thickness

of Nanostructured ZnO Film by Spin Coating Technique," J. Nepal Phys. Soc., vol. 7, no. 2, pp. 119–125, 2021, doi: 10.3126/jnphyssoc.v7i2.38632

[10] R. P. Yadav and K. B. Rai, "Tailoring of ZnO thin films: effect of number of coating and sample ageing," Int. J. Math. Phys., vol. 14, no. 2, pp. 95–102, 2023, doi: 10.26577/ijmph.2023.v14.i2.011

[11] I. Ljubic and A. Sabljić, "Theoretical study of structure, vibrational frequencies, and electronic spectra of dibenzofuran and its polychlorinated derivatives," J. Phys. Chem. A, vol. 111, no. 7, pp. 1339–1350, 2007, doi: 10.1021/jp0676336

[12] S. Y. Lee, "Density functional theory calculation of molecular structure and vibrational spectra of dibenzofuran in the ground and the lowest triplet state," Bull. Korean Chem. Soc., vol. 22, no. 6, pp. 605–610, 2001.

[13] A. A. El-Saady, N. Roushdy, A. A. M. Farag, M. M. El-Nahass, and D. M. Abdel Basset, "Exploring the molecular spectroscopic and electronic characterization of nanocrystalline metal-free phthalocyanine: a DFT investigation," Opt. Quantum Electron., vol. 55, no. 7, pp. 662, 2023, doi: 10.1007/s11082-023-04877-8

[14] S. Kaya and C. Kaya, "A new method for calculation of molecular hardness: a theoretical study," Comput. Theor. Chem., vol. 1060, pp. 66–70, 2015, doi: 10.1016/j.comptc.2015.02.005

[15] M. A. M. El-Mansy, M. S. El-Bana, and S. Fouad, "On the spectroscopic analyses of 3- hydroxy-1-phenyl-pyridazin-6(2H)-one (HPHP): a comparative experimental and computational study," Spectrochim. Acta A Mol. Biomol. Spectrosc., vol. 176, pp. 99–105, 2017, doi: 10.1016/j.saa.2016.12.038

[16] S. Limbu, T. Ojha, R. R. Ghimire, and K. B. Rai, "An investigation of vibrational analysis, thermodynamics properties and electronic properties of formaldehyde and its stretch by substituent acetone, acetyl chloride and methyl acetate using first principles analysis," BIBECHANA, vol. 21, no. 1, pp. 23–36, 2024, doi: 10.3126/bibechana.v21i1.58684

[17] S. Ghafoor, A. Mansha, S. Asim, M. Usman, A. F. Zahoor, and H. S. Ali, "The structural, spectral, frontier molecular orbital and thermodynamic analysis of 2-hydroxy 2-methyl propiophenone by MP2 and B3LYP methods," J. Theor. Comput. Chem., vol. 19, no. 5, p. 2050020, 2020, doi: 10.1142/S0219633620500200

[18] E. M. Alkhateeb and A. A. Elbarbary, "A theoretical study of hydrogen adsorption on surface nanocone materials," Curr. Sci. Int., vol. 7, no. 3, pp. 370–375, 2018.

[19] K. B. Rai, R. R. Ghimire, C. Dhakal, K. Pudasainee, and B. Siwakoti, "Structural equilibrium configuration of benzene and aniline: A first-principles study," J. Nepal

Chem. Soc., vol. 44, no. 1, pp. 1–15, 2024, doi: https://doi.org/10.3126/jncs.v44i1.62675

[20] P. Govindasamy, S. Gunasekaran, and S. Srinivasan, "Molecular geometry, conformational, vibrational spectroscopic, molecular orbital and Mulliken charge analysis of 2-acetoxybenzoic acid," Spectrochim. Acta A Mol. Biomol. Spectrosc., vol. 130, pp. 329–336, 2014, doi: 10.1016/j.saa.2014.03.056

[21] D. Shoba, S. Periandi, S. Boomadevi, S. Ramalingam, and E. Fereyduni, "FT-IR, FT- Raman, UV, NMR spectra, molecular structure, ESP, NBO and HOMO–LUMO investigation of 2-methylpyridine 1-oxide: A combined experimental and DFT study," Spectrochim. Acta A Mol. Biomol. Spectrosc., vol. 118, pp. 438–447, 2014, doi: 10.1016/j.saa.2013.09.023

[22] T. Ojha, S. Limbu, P. M. Shrestha, S. P. Gupta, and K. B. Rai, "Comparative computational study on molecular structure, electronic and vibrational analysis of vinyl bromide based on HF and DFT approach," Himalayan J. Sci. Technol., vol. 7, no. 1, pp. 38–49, 2023, doi: 10.3126/hijost.v7i1.61128

[23] E. A. Bisong, H. Louis, T. O. Unimuke, J. O. Odey, E. I. Ubana, M. M. Edim, F. T. Tizhe, A. Agwupuye, and P. M. Utsu, "Vibrational, electronic, spectroscopic properties, andNBO analysis of p-xylene, 3,6-difluoro-p-xylene, 3,6-dichloro-p-xylene and 3,6-dibromo-p-xylene: DFT study," Heliyon, vol. 6, no. 12, p. e05783, 2020, https://doi.org/10.1016/j.heliyon.2020.e05783

[24] S. K. Ignatov, Moltran v. 2.5 – Program for Molecular Visualization and Thermodynamic Calculations, University of Nizhny Novgorod, 2004.

[25] I. Puigdomenech, A. Joseph, A. V. Plyasunov, and I. Grenthe, "Temperature corrections to thermodynamic data and enthalpy calculations," in Modelling in Aquatic Chemistry, OECD Publications, 1997, ISBN: 92-64-15569-4

[26] V. S. Iorish, O. V. Dorofeeva, and N. F. Moiseeva, "Thermodynamic properties of dibenzo-p-dioxin, dibenzofuran, and their polychlorinated derivatives in the gaseous and condensed phases. 2. Thermodynamic properties of condensed compounds," J. Chem. Eng. Data, vol. 46, no. 2, pp. 286–298, 2001, doi: 10.1021/je000279j

[27] H. R. K. Gauli, K. B. Rai, K. Giri, and R. Neupane, "Monte-Carlo simulation of phase transition in 2D and 3D Ising model," Scientific World, vol. 16, no. 16, pp. 12–20, 2023, DOI: 10.3126/sw.v16i16.56744

[28] A. Pan, A. K. Rakshit, and S. P. Moulik, "Micellization thermodynamics and the nature of enthalpy-entropy compensation," Colloids Surf. A Physicochem. Eng. Asp., vol. 495, pp. 248–254, 2016, doi: 10.1016/j.colsurfa.2016.01.023